Bradys (Nevada) InSAR Anomaly Evaluated With Historical Well Temperature and Pressure Data

Lisa Shevenell[1], Gary Oppliger[2], Mark Coolbaugh[3], and James Faulds[4]

[1]ATLAS Geosciences Inc, and Nevada Bureau of Mines and Geology, Reno NV
[2]Zonge Geophysics, Reno NV
[3]Rennaissance Gold, Reno NV
[4]Nevada Bureau of Mines and Geology, UNR, Reno NV
lisas@atlasgeoinc.com • gary.oppliger@zonge.com
sereno@dim.com • jfaulds@unr.edu

Keywords

Geothermal, Nevada, InSAR, Bradys, temperature logs, upflow, outflow, temperature decreases, pressure decreases

ABSTRACT

In 2005, Oppliger et al. demonstrated a new approach for modeling satellite interferometric synthetic aperture radar (InSAR) observed surface deformations in terms of 3-D subsurface volume-strain rate (change) distributions using the Bradys geothermal field as a case study. A key result was the recognition of volume-strain in shallow lateral horizons to the northwest of the Bradys field indicative of thermal fluid outflow. The model also postulated that the volume decrease for a distance of approximately 5 km away from the main Bradys fault splays could be attributed to temperature and pressure decreases at approximately 1.5 km depth. The temperature and pressure log data presented here validate the presence of a shallow, laterally short outflow plume near the Bradys fault and a zone of decreased temperature and pressure away from the fault at about 300 to 600 m. While shallower than the postulated 1.5 km depth, that depth was modeled without any physical constraints on pressure and temperature in the reservoir. These data were only used to validate the model, which could now be calibrated given the close match between observed and modeled results.

Introduction

In 2005, Oppliger et al (2005) demonstrated a new approach for modeling interferometric synthetic aperture radar (InSAR) at geothermal systems under production, using Bradys, Nevada as a test case. In that work, Oppliger was able to show reservoir boundaries through subsidence signatures and model for lateral outflow contributions to the InSAR pattern, suggesting that the reliability of reservoir geometric modeling can be improved using InSAR and complementary data sets. Reservoir boundaries were identified through the InSAR scenes, since flow barriers (impermeable fault segments) channel the outflow and show as distinct edges to the InSAR anomalies. It was postulated that changes to flow rates may further reveal these structures. Also, part of the outflow may contribute to the field's short-term self-recharge by becoming downward convective return flow in distal segments of the Bradys fault zone. By understanding these patterns, it is possible to improve placement of reinjection wells to optimize the resource.

In the previous work, several hypotheses were suggested to explain the observed InSAR signatures, one of which suggested a thermal anomaly trending NW from the main subsidence feature (Oppliger et al., 2005, and Figure 2 below). It was postulated that temporal changes in temperature or pressure in lateral outflow zones above the main production zones may make a significant contribution to the observed InSAR and should be accounted for in future modeling efforts. The purpose of this work is to test the hypothesis that the observed InSAR anomaly can be validated using temporal well temperature and pressure logs over similar time intervals and determine if, indeed, the observed and modeled anomaly is a reflection of the presence of a lateral outflow in the subsurface trending northwest from the main subsidence signature.

Background

The Bradys field is a geothermal system currently has a production capacity of approximately 26 MW that first came on-line in 1992 and is still producing power today. The location of this field in Nevada is shown in Figure 1.

Previous work by Oppliger et al. (2005) investigated the relation between geothermal reservoir compaction (or bulk porosity loss), geometry and production rates by recovering a ten-year InSAR ground displacement history at the Bradys and Desert Peak fields. In this previous study, the authors found an anomaly within the InSAR signature that was modeled to be consistent with a lateral outflow zone exhibiting a zone of decreased temperature or pressure as a result of production. A key conclusion derived from the previous work is that the model reflects changes in temperature and/or pressure in upper lateral outflow zones. These changes make a significant contribution to the observed InSAR patterns and must be modeled in combination with the operational

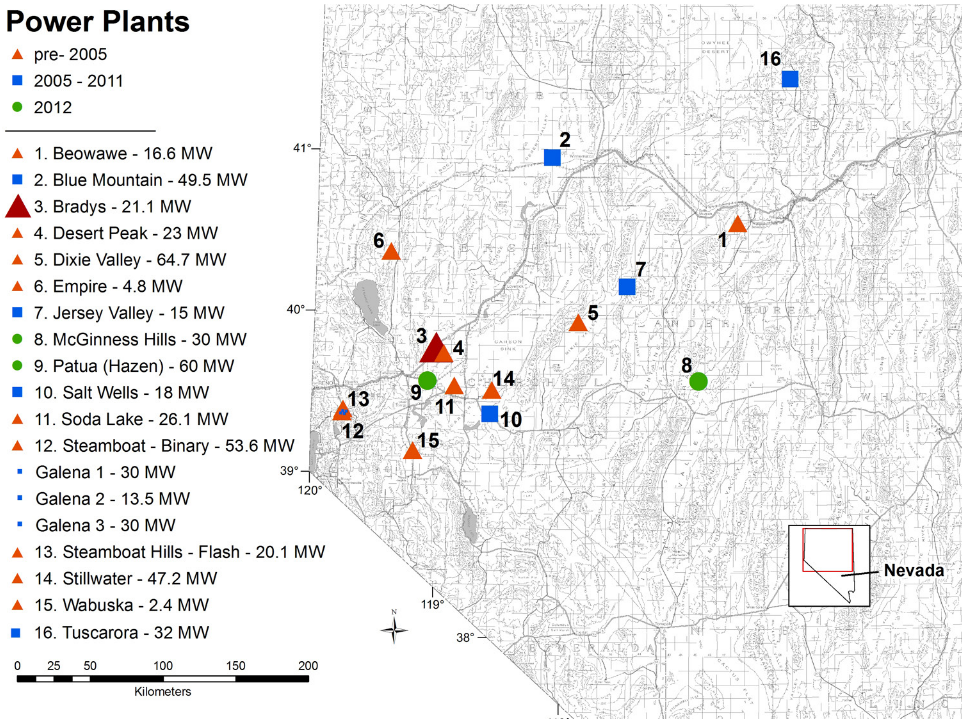

Figure 1. Locations of active geothermal power plants in Nevada. Bradys is located at position #3 at the large red triangle. MW values are nameplate capacities rather than gross or net generation in any given year.

reservoir to fully understand the reservoir geometry and impacts of commercial production.

The geothermal potential of Nevada thermal areas has long been known. In particular, the numerous hot springs across Nevada first drew Native Americans to hunt the wildlife that lingered nearby. Later, the geothermal area at Bradys drew travelers. Those springs lured pioneers on their long westward trek with the promise of hot water for cooking and bathing. Steam rising near Bradys Hot Springs about 50 miles northeast of Reno attracted early pioneers who called the area the "Spring of False Hope." Journals recount how oxen that pulled wagon trains could smell the moisture before reaching the springs, and would speed up to reach the enticing water—only to find that the water was scalding hot and undrinkable (Benoit et al., 1982). Thermal features at Bradys show groundwater discharge from the thermal area is in part by evaporation/boiling through a series of fumaroles, and through lateral subsurface outflow at various depths.

The pre-production state of the Bradys geothermal field included convective up-flow as evidenced by its historic hot spring flows and fumaroles (Benoit et al., 1982), which could potentially supply horizontal outflow.

This allows the possibility that both the reservoir and outflow systems could experience production related perturbations in temperature, pressure and flows rates that may be expressed in InSAR observations. The Bradys field has been studied and mapped in detail in recent years, with new mapping showing the surface traces of multiple fault traces in relation to thermal features, such as springs, fumaroles, warm ground, and sinter (Faulds et al., 2010, unpublished data).

Oppliger et al. (2005) speculated that the modeled and observed volume-strain patterns may be produced from changes in geothermal fluid outflow into the upper adjacent aquifer system, which result in minor temperature or pressure decreases. The ~250 meter thick thermal aquifer (Figure 2) modeled by Oppliger et al. (2005) is essentially shrinking at a rate of 9 ppm/year, which is consistent with a ~0.33ºC/year temperature reduction. If the effective aquifer model thickness were changed to 500 meters, the required temperature decrease would be only 0.15 ºC/year. These modeled temperature decreases in this InSAR compatible reservoir volume-strain rate model represent the maximum possible temperature changes in the hypothetical aquifer system, because pore pressure decrease associated with reduced outflow would also almost certainly account for some of the observed aquifer volume losses depicted in the InSAR scenes.

Wells from the Brady fault zone and the area to the NW are investigated to determine if there is a lateral outflow zone as depicted here or if changes in temperature and pressure may account for the long wavelength feature highlighted above. Oppliger's (2005) A-A' section is at the approximate location of the C-C' section in this paper in Figure 3, and in Faulds (unpublished data). InSAR model strike length is 4.8 km perpendicular to the cross-section. No vertical exaggeration.

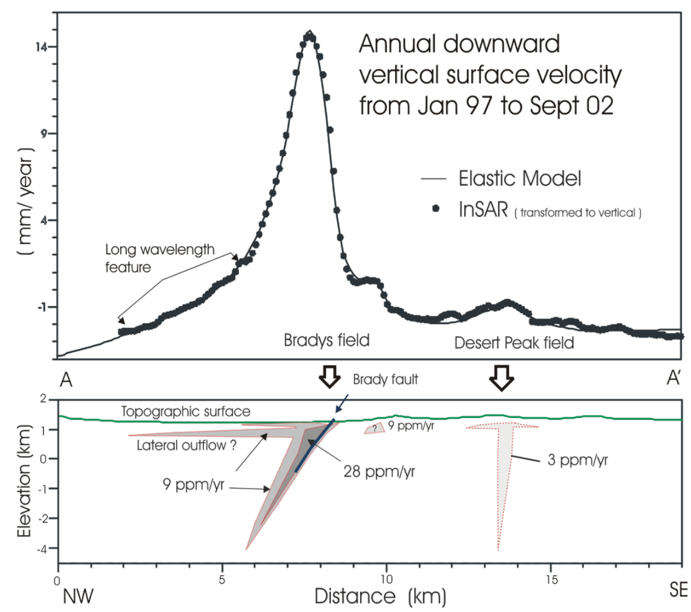

Figure 2. Modeled InSAR anomaly (Bradys model) from Oppliger et al. (2005), with only minor modifications. The top diagram shows the InSAR profile across cross-section C-C′ of Figure 3 and the bottom diagram shows the modeled interpretation of the InSAR data. The long wavelength surface deformation feature on the extreme left (northwest) part of the profile indicates significant volume-strain is occurring in that area somewhere between the surface and about 1.5 kilometers depth.

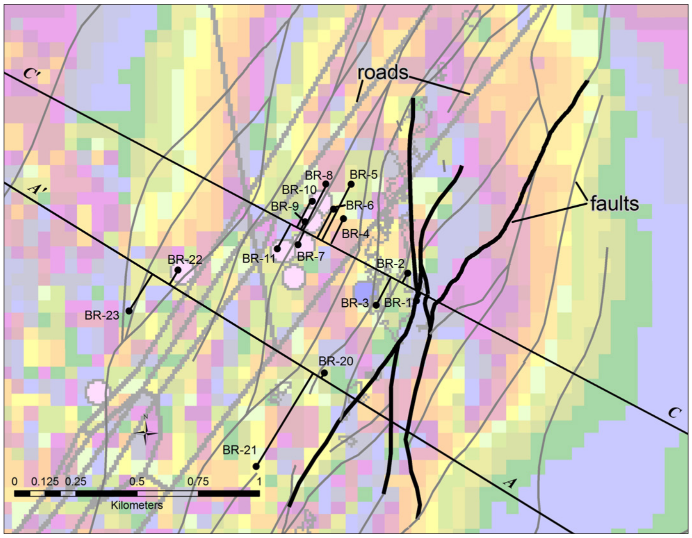

Figure 3. Map showing well locations (numbers) discussed in the text. The InSAR anomaly from Oppliger et al. (2005) is the gradational colors in the background, and the lines are faults by Faulds et al. (2010; 2012, unpublished). Bold lines are faults in the area of the main Bradys fault zone. Section C-C′ above is at the approximate location of the cross section on Figure 2 (from Oppliger et al., 2005), and at the same location as the one constructed by Faulds et al. (2012, unpublished). Cross section A-A′ was selected in this work for its proximity to the anomaly noted in Figure 2. The numbers at the dots are well identifiers noted in tables and figures below (labeled BR-1, BR-2, etc.), showing a leader to the cross-section line on which they are projected.

Table 1. Summary of wells at Bradys for which data were available and evaluated in this study. Locations depicted in Figure 3.

Well Number	Spud Date	Date Completed	TD	1st Date Pumped*	Date Inject*
BR-1	12/04/91	12/19/91	2500	--	--
BR-2	04/19/74	10/04/74	7275	--	--
BR-3	11/08/91	12/14/91	1999	P&A	--
BR-4	10/14/90	11/01/90	3011	--	--
BR-5	08/15/91	09/13/91	2404	--	--
BR-6	09/18/91	09/30/91	1206	--	--
BR-7	11/13/91	11/25/91	1920	2002	pres
BR-8	10/30/91	11/13/91	1979	--	--
BR-9	11/01/91	11/30/91	1938	2002	2002
BR-10	11/16/91	11/30/91	2000	2002	2007
BR-11	12/05/91	12/19/91	2325	2002	2004
BR-12	09/20/97	11/01/97	4301	--	--
BR-20	10/1/1985	10/20/85	623	--	--
BR-21	11/6/1964	12/10/64	5062	--	--
BR-22	7/14/1996	07/15/96	3037	2002	2009
BR-23	3/25/1963	04/30/93	4089	--	--

* Note: pumping records are not reported for individual wells by the Nevada Division of Minerals (DOM) prior to 2002. The dates above for pumping and injection only reference the first year in which the records are reported by DOM.

Methods

Temperature and pressure logs at the location of the numbered dots of Figure 3 were obtained by the operators at the Bradys geothermal site and compiled and plotted to determine several conditions. The logs were used to evaluate if they were located in an upflow or outflow zone to the geothermal system. Changes through time were evaluated to determine if production had altered either the temperature or pressure signatures in the cases where these data were available both before and after initial operations began. The locations of the available well logs are plotted along cross sections spatially (and temporally) in relation to the observed InSAR subsidence signatures. The patterns and changes along the two cross sections illustrated in Figure 3 were evaluated to help explain the modeled InSAR anomaly presented in Oppliger et al. (2005). Summary of the wells in these two cross sections are listed in Table 1.

Temperature reversals were used to identify lateral outflow zones at different depths (e.g., see Fig. 5 BR-3 at about 400 ft depth), whereas the typical signature of upflow zones (broad upward curve of high, shallow gradient, e.g., see Figure 4, BR-1) was used to locate changes in the flow system from upflow to outflow. Pressure changes in the available well logs were also investigated to determine the impact these changes might have on the observed and modeled InSAR signatures. Note that the post completion pressure logs were obtained in cased holes such that the information simply shows hydrostatic conditions in the well based on the pressure in the completion zone at the time of measurement. Hence, pressure changes in the lateral outflow zones cannot be directly determined, but an evaluation of overall pressure decreases in the reservoir following initiation of production can be made.

Results

Figure 3 shows the locations of the cross sections evaluated in this work that correspond with the approximate location of the modeled anomaly in Figure 2, reproduced from Oppliger et al. (2005). There are 19 wells with temperature and pressure logs in the vicinity of the Bradys fault zone and modeled InSAR anomaly (depicted in Figure 3; well numbers were changed to BR-1, 2, 3 etc. per request of the current operator, Ormat,). Well logs are presented in order from southeast to northwest away from the main segment of the Bradys fault to locate outflow zones and their depth. These results are compared to the InSAR modeling results of Oppliger et al. (2005) in the Discussion section. Well numbers appear on Figure 3 in relation to mapped faults in the study area (after Faulds et al. (2012, unpublished)).

Well BR-1 – Section C-C′

Both temperature (Figure 4) and pressure logs (not depicted here) indicate that this well is at or near the upflow area in the Bradys fault zone as depicted by the broad curve with steep, shallow gradients, with decreasing gradients in the lower part of the profile. Temperature logs are available for two dates, both shortly after the well was completed on 12/19/91. The log from 1/9/92 was apparently not fully equilibrated as the overall temperature increased, resulting in the log from 3/29/92. No later logs following initiation of field production were available as part of this work, but the pre-production information indicates this well is near a fault along which there is geothermal fluid upflow. The first pressure log (not depicted) also suggests that the well is in an upflow zone (showing the same pattern), but the second available log was run in a cased hole and shows a constant increasing pressure with depth, so no pressure changes with time can be discerned.

Well BR-2 – Section C-C′

Permitted well data collected by the Nevada Division of Minerals (DOM) and compiled into a database by the Nevada Bureau of Mines and Geology (NBMG) indicate that this well was completed in October 1974 to a depth of 7,275 ft (2,217 meters), yet the log of Figure 4 shows that four of the static logs were run before well completion (to total depth with consistent temperature increase with depth not illustrated on Figure 4), and two after, although only to a depth of 2,430 ft (761 m). This log illustrates a number of irregularities including a very large (currently unexplained) temperature decrease in the logs from 11/9 to 11/13/85 (red to purple in only four days), with apparent thermal inflow zones at 89 and 1,070 ft (27 and 326 m). However, both early logs (two in July, 1974) show a possible temperature reversal at 500 ft, which apparently had smoothed out by 1985. An outflow zone at 250 ft (76 m) is indicated in the 11/9/85 log, which may have been present in the 1974 logs had they been logged at sufficiently dense spacing. All logs depicted in Figure 4 were obtained before initiation of field production. The log from 11/9/85 is considered to be the most reliable for the given purpose in this paper and shows a shallow temperature outflow zone at approximately 250 ft (76 m). An increase at about 1800 ft (550 m) is also evident suggestive of another possible lateral flow zone at depth.

Well BR-3 – Section C-C′

Figure 5 shows BR-3 and -4, where well 3 was completed 12/14/91 and showed increasing temperature with time until apparent equilibration on 3/27/92. Both post-completion logs indicate a thermal fluid outflow zone at approximately 360 ft (110 m), with a slight increase in depth seen in the later log (3/27/92). All available pressure logs were obtained prior to initiation of production of the field and show consistent increases with depth.

Well BR-4 – Section C-C′

The pattern depicted in Figure 5 indicates an upflow zone, with increasing temperatures as the well equilibrated after completion on 11/1/90. The well was mostly equilibrated as of 12/7/90, showing a similar profile as was measured on 2/1/94, slightly over three years after completion. No apparent change in temperature occurred in this well as a result of initiation of field production in 1992. No appreciable pressure changes were observed in the well that might indicate changes in the flow near this well as a result of initiation of field production in 1992.

Well BR-5 – Section C-C′

Figure 6 shows BR-5 and -6, with BR-5 having been completed on 9/13/91. All depicted logs indicate this well is in an upflow zone with a thermal outflow zone at approximately 1,050 ft (320 m) indicated in the one log (10/19/91) that extends to sufficient depths. No appreciable pressure changes were observed in the well that might indicate changes in the flow near this well, although no logs are available following initiation of production of the field.

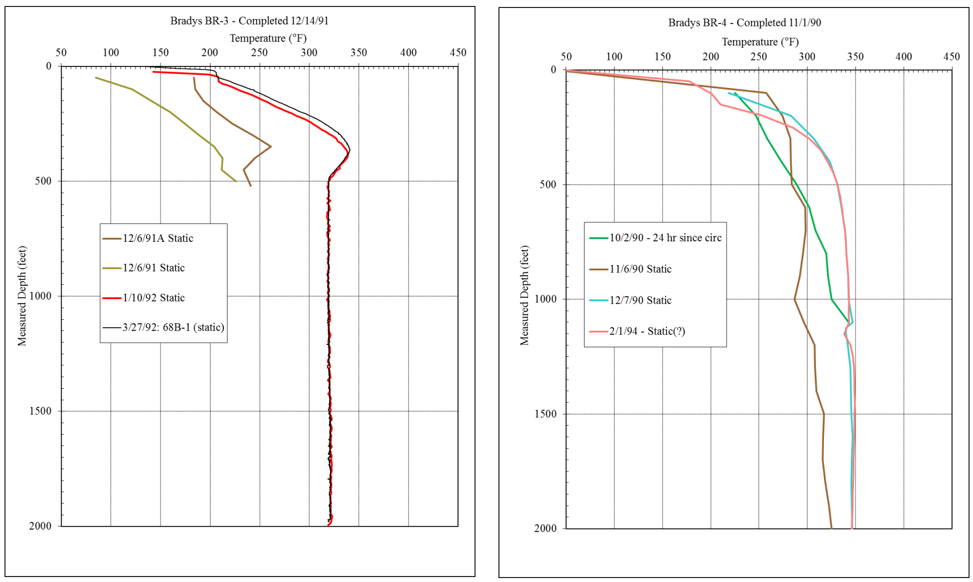

Figure 5. Temperature logs for (a) BR-3 and (b) BR-4 (locations depicted on Map of Figure 2).

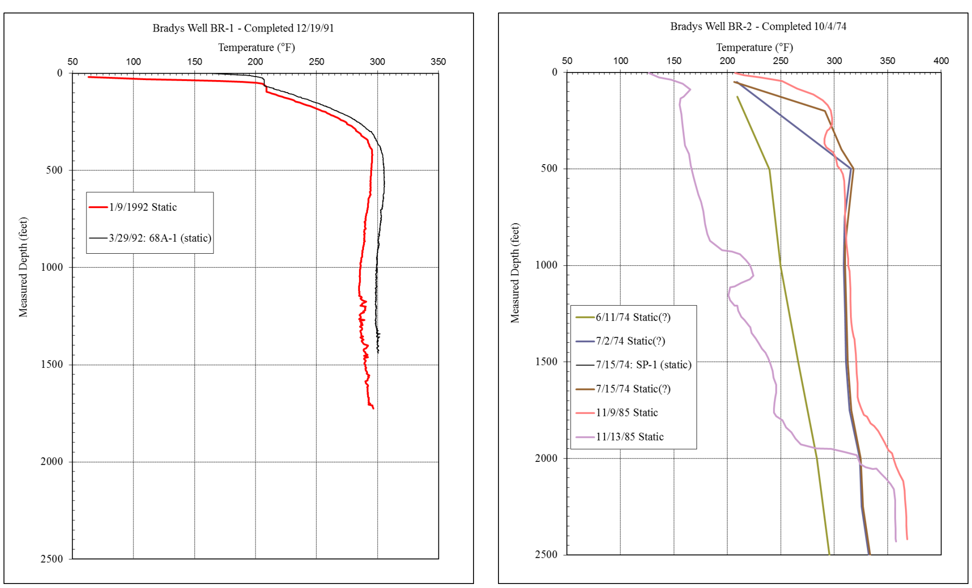

Figure 4. Temperature logs for (a) BR-1 and (b) BR-2. Locations depicted on Figure 3.

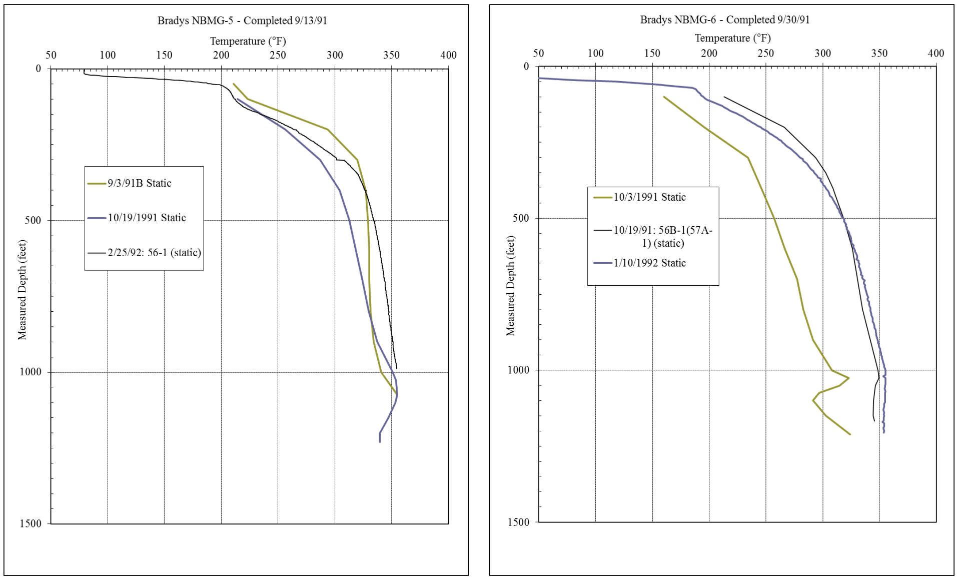

Figure 6. Temperature logs for (a) BR-5 and (b) BR-6 (locations depicted on Map of Figure 2).

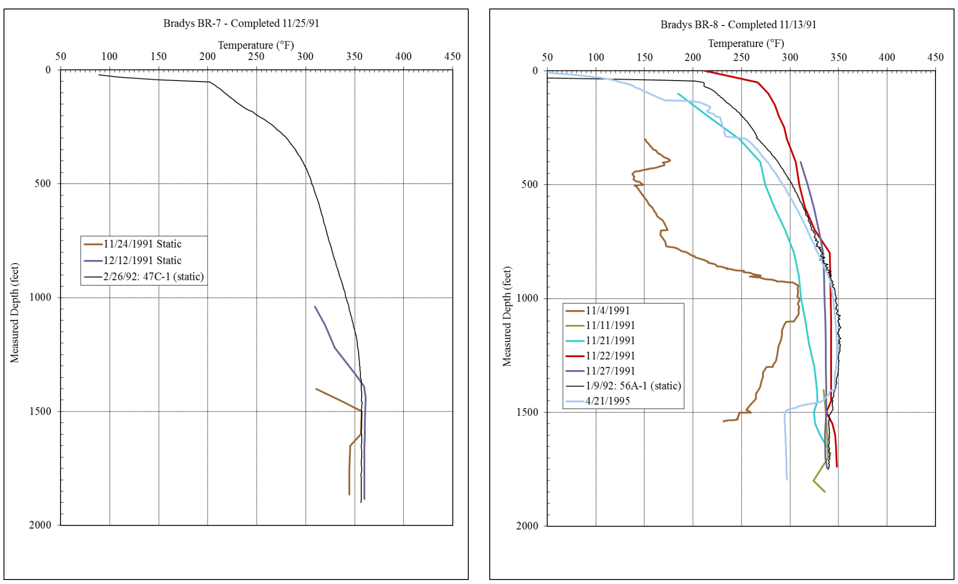

Figure 7. Temperature logs for (a) BR-7 and (b) BR-8 (locations depicted on Map of Figure 2).

Well BR-6 – Section C-C′

This well was completed 9/3/91, with the first temperature log obtained one month later on 10/3/91. A consistent increase in temperature is depicted in the well through 1/10/92, which shows the well is in an upflow zone (Figure 6). No appreciable pressure changes were observed in the well that might indicate changes in the flow near this well, although no logs are available following initiation of production of the field.

Well BR-7 – Section C-C′

This well was completed on 11/25/91, with the equilibrated temperature log having been obtained on 2/26/92, which shows the typical pattern of an upflow zone (Figure 7). This well ultimately became a production well. Pressure logs show a consistent increase with depth, although only two logs were available (12/12 and 12/13/91)

Well BR-8 – Section C-C′

The temperature log for BR-8 (Figure 7) shows some variability over time but generally shows this well is also in an upflow zone. This well was completed 11/13/91 and indicates that the well may have been equilibrated relative to temperature by 11/22/91. A relatively large temperature decrease (40-50°F) in the upper part of the well is observed by 4/21/95 compared to the 11/22/91 date, suggesting initiation of production at the site impacted this particular well. Pressure logs also indicate a decrease between 11/7/91 and 4/21/95 as a result of nearby production. Pressure in the bottom of the well decreased by approximately 40 psig.

Well BR-9 – Section C-C′

This well was completed 11/30/91, and Figure 8 depicts several temperature logs indicative of an upflow zone at this well. The well had equilibrated by 1/8/92, and temperatures began to decline by 11/4/94, further decreasing by the last date depicted on 8/13/95, which is not surprising given that this is a production well. The temperature decrease observed in this well was approximately 51°F (28.3°C at 1000 ft; 305 m) as a result of production. Possible outflow was initiated at about 100 ft (30.5 m) as depicted on the 11/4/94 and 8/13/95 logs.

Pressures were also seen to decrease in this well near the bottom of the hole (1600 ft) between 1/8/92 and 8/14/95. After development began in 1992, this well exhibited a 73 psig decrease in pressure, which is not surprising given that this well was noted to be a production well after 2002, and likely before that time.

Well BR-10 – Section C-C′

This well was also completed 11/30/91, with the logs in Figure 8 also showing this well is in an upflow zone. This well is noted by the DOM data to be a production well in 2002 (when records began) and an injection well as of 2007, and hence, changes in temperature and pressure with time are to be expected in this well. The well was clearly not equilibrated with respect to temperature when the first log was run on 12/5/91, increased to an equilibrated level by 1/8/92 and decreased in two parts of the well by 5/9/94. A 23°F (18.3°C) decrease at 500 ft and a 20°F (11.1°C) decrease at 1,500 ft (457 m) were observed over this 2.3 year period.

Similarly, the pressure was measured on 12/5/91 and appears to be equilibrated as the trace overlies the log obtained on 1/8/92. In the following 2.3 year period to 5/9/94, the temperature near the bottom of the hole (at 1600 ft; 488 m) decreased by 36 psig.

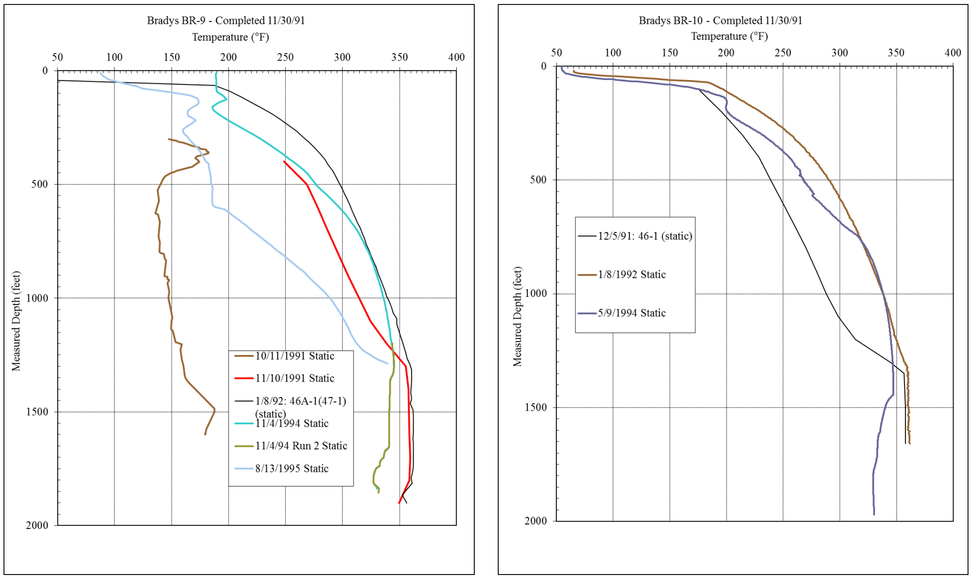

Figure 8. Temperature logs for (a) BR-9 and (b) BR-10 (locations depicted on Map of Figure 2).

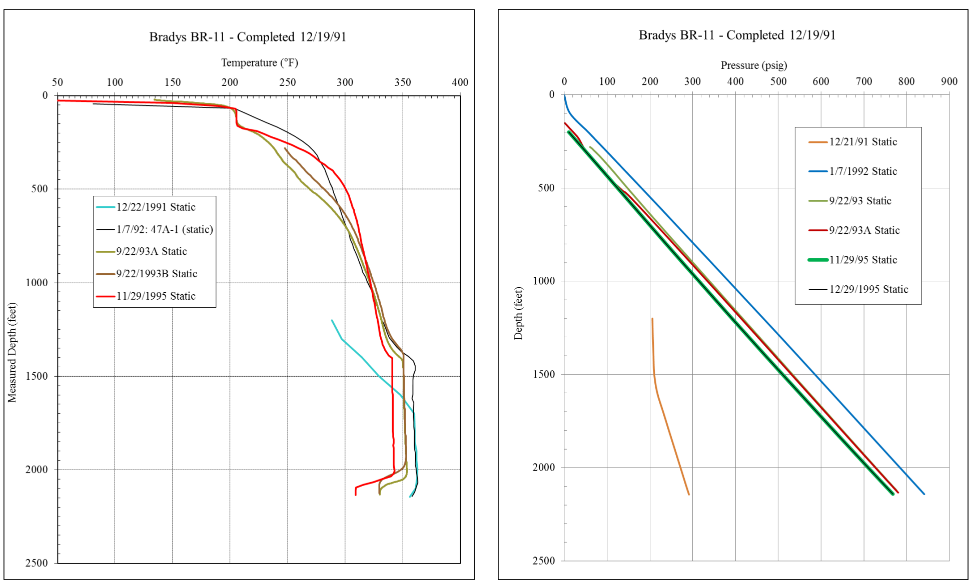

Figure 9. Temperature (a) and pressure (b) logs for BR-11 (location depicted on Map of Figure 2).

Well BR-11 – Section C-C′

This well also exhibits the typical signature of an upflow zone (Figure 9), and although it was only completed 12/19/91, it appeared to have reached equilibrium by 1/7/92. DOM records indicate that this was a production well producing fluids in 2002, and an injection well in 2004, so perturbations in the well log temperatures with time are to be expected. The logs showed a small increase in temperature (11°F, 6.1°C) at 500 ft (152 m), and a decrease of 19.5°F (10.8°C) at 2,000 ft (610 m) with increasing time.

Similarly, the pressure seemed to have stabilized by 1/7/92 and decreased with time until 12/29/95, with an overall 74 psig decrease at 2,000 ft (610 m).

Well BR-20 – Section A-A′

This well was completed on 10/1/85 and shows two distinct outflow zones in most logs at approximately 74 ft and 430 ft (22.6 and 131 m). It appeared to have equilibrated by 2/1/86, slightly over 3 months following completion (Figure 10). A temperature decrease of 52°F (29.2°C) occurred between 3/27/92 and 4/18/94 at the maxima of the temperature reversals, although the peak in the reversal migrated upward by 18 ft (5.5 m) by 4/18/94. Pressure decreased over the same time period by 32 psig at 400 ft (122 m), and a similar decrease to the total depth (TD) of the well is anticipated as the logs are nearly parallel, though not all were run to TD.

Well BR-21 – Section A-A′

This well also intersects an outflow plume as seen in three of the logs in Figure 10. The well was completed 11/6/64, with the first logs available on 2/3 and 2/9, 1978. The three logs that show temperature overturns were recorded 2/3/78, 2/9/78 and 2/26/92, which suggest a general downward movement of the maximum in the temperature reversal from 500 ft to 658 ft (152 to 200.6 m). There were variations in temperatures with the 2/3/78 log showing 246.4°F (119.1°C), 306°F (152°C) on 2/9/78 and 293.6°F (145°C) on 2/26/92. Hence, there appeared to be a sharp increase in temperature after six days in 1978 (59.6°F; 33.1°C), but a later decrease on 2/26/92 to 293.6°F (145°C) (a decrease of 12.4°F (6.9°C) from 2/9/78). Only one pressure log is available (on 2/26/92), and no temporal changes can be evaluated.

Well BR-22 – Section A-A′

This well was completed on 7/15/96. Three logs were run, all shortly after shut-in, but no date was available with the data to determine how long after completion the logs were run (Figure 11). The logs suggest that the well occupies a possible upflow zone (although the main indication was recorded only 28 hrs after well shut-in). All three logs show a temperature spike at 2648 ft of 243°F (117.2 m) that could be a narrow outflow plume, although it seems unlikely given the location/depth of the other outflow zones noted in the area. No pressure data were available.

Well BR-23 – Section A-A′

This well was completed 4/3/93 and had 4 available temperature logs that show a continuous increase (no convective flow indicated) in temperature at all depths to 3,000 ft (where all logs show temperatures <350°F; <176.7 m) between 5/7/93 and 8/14/95

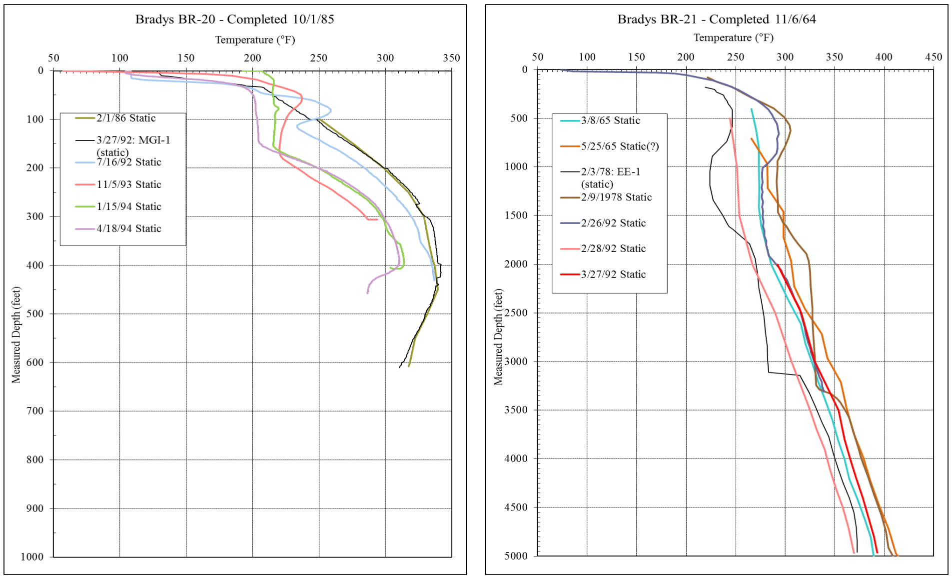

Figure 10. Temperature logs for (a) BR-20 and (b) BR-21 (location depicted on Map of Figure 2). Note that both the vertical and horizontal scales of the two logs differ significantly.

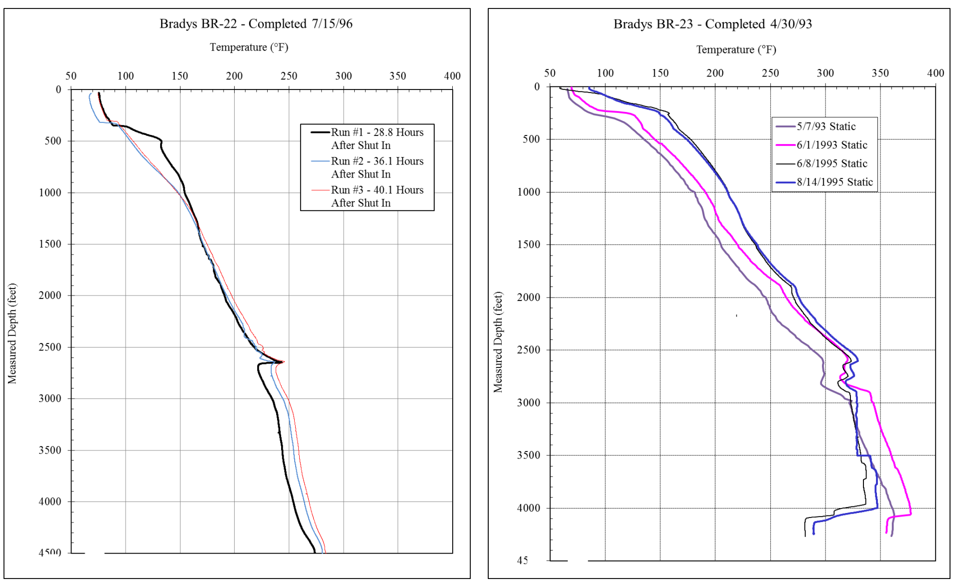

Figure 11. Temperature logs for (a) BR-22 and (b) BR-23 (location depicted on Map of Figure 2).

(Figure 11), indicating nearby injection was likely impacting this well during early production. Below 3,500 ft (1067 m), the signatures are more erratic showing temperatures decreased in the following order: 6/1/93 to 5/7/93 to 6/8/95, increasing slightly in 8/14/95. No pressure logs were available

Discussion

The Bradys field InSAR pattern contains a number of narrow width anomalies, which were interpreted as caused by fault plane flow barriers. Since these narrow wavelengths require sources in the upper 328 to 656 ft (100-200 m), it was postulated that lateral outflow, evidenced primarily by a "long wavelength feature" of Oppliger et al.,2005 (see Fig. 2), was occurring at this shallow level based on modeling of the InSAR anomalies. Although most of the wells for which there are data along the section of the anomaly indicate the wells tap upflow zones rather than lateral outflow zones, two close to the fault indicate outflow at shallow depths. Wells BR-2 and -3 located along the C-C' line close to the main fault splays (Figure 12) show outflow plumes at 250 and 360 ft depth (76 and 110 m), respectively, which matches the InSAR modeling quite well (100 to 200 m). Other wells (BR-20, -21) near the main fault splay, but toward the south on section line A-A', also provide evidence of lateral outflow away from the Bradys fault zone toward the NW at 430 and 500 ft (131 and 152 m), again fitting quite well with the model results presented previously by Oppliger et al. (2005).

An additional sub-horizontal tabular volume-strain source extending about 5 km northwest of the Bradys reservoir in the upper 1.5 km is one physically plausible model postulated by Oppliger et al. (2005). This hypothesis accounts for the observed long wavelength asymmetry, and it was speculated that this lateral tabular volume-strain feature was an indication of production induced change in the field's lateral outflow patterns that had resulted in small temperature and/or pressure reductions in these areas. The data presented here show no outflow zones away from the main fault splay, but rather upflow (where well data are available). However, four of the wells along C-C' (BR-8, -9, -10, and -11) all exhibit temperature and pressure decreases following initiation of production in 1992. The temperature decreases range from 20 to 51°F (from 1000 to 1750 ft (305 to 533 m), depending on the well), whereas the pressure decreases range from 36 to 74 psig (from 1600 to 2000 ft (488 to 610 m), depending on the well). Hence, the postulated cause of the lateral tabular volume-strain feature by Oppliger et al. (2005) is verified by the presented data. Note that it is likely that other wells in this zone may exhibit temperature and pressure decreases following production, but they are not noted here because some wells had no available measurements following initiation of production and some did not have multiple logs from which to make such a determination.

Conclusions

Although timing of the availability of the well log data and InSAR scenes differs, the well log and InSAR data both show the general patterns in the reservoir that occurred in the past and likely persist into the present, although the magnitudes are likely to vary with time. In spite of this timing limitation, the model

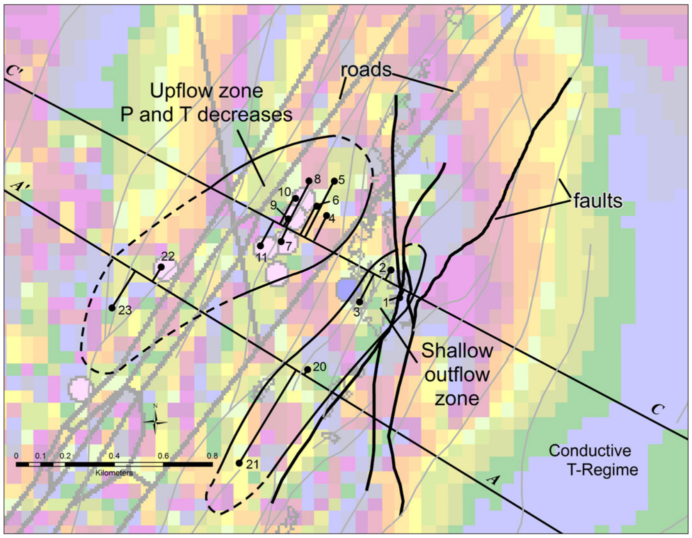

Figure 12. Bradys map showing locations of wells discussed in this paper and a general depiction of flow regimes based on available temperature data.

using InSAR pairs presented by Oppliger et al. (2005) matches observed temperature log data and interpreted reservoir configuration remarkably well. This good match was made without the benefit of having had temperature log data. The InSAR model was not biased by any temperature and pressure log data in the model formulation. The InSAR model detected a shallow, short outflow plume near the main surface traces of the Bradys fault quite well where the actual depths noted of the outflow detected in the wells were between 76 and 110 m, whereas the model predicted the depth of the outflow feature at 100 to 200 m, well within the observed range.

The model was also capable of detecting a lateral tabular volume-strain feature that was reflected by measured pressure and temperature, and hence volume, decreases observed in the wells between 300 and 610 m. This depth is shallower than the postulated depth of the InSAR modeled feature, which indicated pressure and temperature reductions at 1.5 km under the particular conditions modeled following initiation of production at the field. However, the model fit to the InSAR data are non-unique and the 1.5 km depth was only one such plausible model. Data obtained at Bradys may be used in the future to help calibrate similar models given the known actual depths and magnitudes of the pressure and temperature decreases as a result of production of the geothermal field. Evaluation of InSAR data was also very useful in delineating different parts of the flow system without the benefit of well data, but which was later verified using such well data.

Acknowledgments

Partial funding for this work was provided via salary support by ATLAS Geosciences Inc and Nevada Bureau of Mines and Geology. This material is partially based upon work supported through four projects by the U.S. Department of Energy under instrument number DE-FG07-02ID14311 to the authors. The first author wishes to thank Andy Sabin (Navy Geothermal Program Office) for helpful review comments, and Thomas Dozet for assistance with the maps and figures.

References

Benoit, W.R., J.E. Hiner, and R.T. Forest, 1982. "Discovery and geology of the Desert Peak geothermal field: A case history." Nevada Bureau of Mines and Geology Bulletin 97, 82 p.

Faulds, J.E., Coolbaugh, M.F., Benoit, D., Oppliger, G., Perkins, M., Moeck, I., and Drakos, P., 2010. "Structural controls of geothermal activity in the northern Hot Springs Mountains, western Nevada: The tale of three geothermal systems (Brady's, Desert Perk, and Desert Queen)." Geothermal Resources Council *Transactions*, v. 34, p. 675-683.

Faulds, J. L. Garside, A. Ramelli, and M. Coolbaugh, 2012 (in prep). "Preliminary geologic map of the Desert Peak-Bradys geothermal fields, Churchill County, Nevada." Nevada Bureau of Mines and Geology Map.

Oppliger, G., M. Coolbaugh, L. Shevenell, and J. Taranik, 2005. "Elucidating deep reservoir geometry and lateral outflow through 3-D elastostatic modeling of satellite radar (InSAR) observed surface deformations: An example from the Bradys geothermal field." Geothermal Resources Council *Transactions*, v. 29, p. 419-424.